Korean J. Chem. Eng., **28**(12), 2282-2286 (2011)
DOI: 10.1007/s11814-011-0125-2

Co-methanation of CO and CO_2 on the Ni_X-Fe_{1-X}/Al_2O_3 catalysts; effect of Fe contents

Suk-Hwan Kang*, Jae-Hong Ryu*, Jin-Ho Kim*, Seok-Jung Seo*, Yong-Done Yoo*†, Potharaju S. Sai Prasad, Hyo-Jun Lim***, and Chang-Dae Byun*****

*Plant Engineering Center, Institute for Advanced Engineering (IAE), Suwon 443-749, Korea
**Inorganic & Physical Chemistry Division, Indian Institute of Chemical Technology, Hyderabad 500 607, India
***POSCO, POSCO Center, 892 Daechi4-dong, Gangnam-gu, Seoul 135-777, Korea
(*Received 4 March 2011 • accepted 9 May 2011*)

Abstract–The co-methanation of carbon dioxide containing syngas was carried out on Al_2O_3 supported Ni_xFe_{1-x} (x is 0.1, 0.3, 0.5, 0.7 and 0.9) catalysts for synthetic natural gas (SNG) production. The catalysts were prepared by wet-impregnation method taking 20 weight percent of the metallic component over the support, and its characteristics were analyzed by BET surface area, XRD and H_2-TPR. The maximum carbon conversion and CH_4 selectivity are achieved on $Ni_{0.7}Fe_{0.3}/Al_2O_3$ catalyst. Further, increase of Fe content led to enhancing the water gas shift reaction and hydrocarbon formation.

Key words: Methanation, Synthetic Natural Gas, Ni-Fe Catalyst, Syngas

INTRODUCTION

During the energy crisis in the 1970s, methanation of synthesis gas from naphtha and coal was considered for manufacture of synthetic natural gas (SNG). This was also stimulated by the shortfall of natural gas supplies [1,2]. However, after a few industrial plants were built, the thrust on SNG synthesis decreased as the energy prices stabilized at a relatively low level during the 1980s [3]. Recently, methanation has regained its importance as an option not only for cleanup of reformates to get hydrogen fuel for low temperature fuel cell, but also to make coal (or biomass) conversion process more economical, particularly when the oil resources are predicted to be limited and energy security is threatened [4,5].

For methanation of syngas containing CO (or CO_2) and H_2, Co- and Ru-based catalysts are known to be more active than the Ni, but they are significantly more expensive [6,7]. Fe is usually much less active and more prone to carbon deposition [8]. Therefore, until now Ni supported on aluminum oxide has been used as a traditional catalyst for methanation [9,10] and is well described experimentally and theoretically [11,12]. In addition, Ni-Co [13] and Ni-Zr catalysts supplemented by rare earth elements such as yttrium, cerium and samarium are found to be effective in the methanation rate of carbon dioxide [14]. Some investigators have reported new and improved bimetallic Ni-Fe catalysts [15] and noble and base metal catalysts supported on zirconia and ceria [16] for methanation.

The methane yield in methanation processes is closely related to the temperature control in the reactor. A typical multi-stage adiabatic reaction system utilizing Ni-based catalysts was reported in the TREMP™ (Topsøe Recycle Energy-efficient Methanation) process, wherein the generated heat in the reactor was used to pre-heat the feed syngas at high space velocity obtained by the recirculation [17]. Even after controlling the methanation process at low temperature in the reactor, some CO_2 was always produced by the WGS (water gas shift) reaction due to equilibrium. However, for increasing the concentration of methane and decreasing the concentration of hydrogen the presence of CO_2 is required. That is why in many commercial SNG processes the investigators proposed connecting a number of adiabatic reactors. Especially, the progress of CO_2 hydrogenation is a key step in the process [18].

In the present work, we performed methanation using the bimetallic catalysts taking the model gas mixture that included CO_2 and related to that of the second adiabatic reactor of TREMP™. The Al_2O_3 supported bimetallic Ni-Fe catalysts with different Fe contents were prepared by wet-impregnation method and we studied the co-methanation of CO and CO_2. The properties of the catalysts were further substantiated by characterization tools such as surface area measurement, XRD and H_2-TPR. The objective of this work is to optimize the Ni/Fe composition in the catalyst to obtain maximum methane selectivity during the hydrogenation.

EXPERIMENTS

1. Catalyst Preparation

The Ni-Fe/Al_2O_3 catalysts were prepared by the conventional wet-impregnation method with γ-Al_2O_3 used as the support. The support was obtained by calcination of the alumina in boehmite phase (high purity of Catapal-B Condea) at 600 °C for 5 h in air. Aqueous nickel nitrate and iron nitrate solutions, in accordance with the given compositions, were mixed thoroughly. The impregnation of the alumina was carried out using these mixtures with continuous stirring at room temperature for 12 h. The sample was then dried in a rotary evaporator before subjecting it for calcination at 500 °C in air for 5 h. The ratio of nickel/iron metal component to that of the alumina in the finished catalyst was fixed at 20/100 by weight. The catalysts are represented as Ni_xFe_{1-x}/Al_2O_3, where x denotes weight ratio of Ni/(Ni+Fe) as 0.1, 0.3, 0.5, 0.7 and 0.9.

2. Catalyst Characterization

The BET surface areas were estimated from nitrogen adsorption isotherm data obtained at temperature of −196 °C on a Micromer-

†To whom correspondence should be addressed.
E-mail: ydnyoo@iae.re.kr

itics, ASAP-2400 equipment. The calcined samples were degassed at 300 °C in a He flow for 4 h before the measurements. The pore volumes and pore size distributions of the samples were determined by the BJH (Barett-Joyner-Halenda) model from the data of the desorption branch of the nitrogen isotherms. The pore volumes were determined at a relative pressure (P/Po) of 0.99.

The powder X-ray diffraction (XRD) patterns were obtained with a Rigaku diffractometer using Cu-K_α radiation to identify the phases of Ni_xFe_{1-x}/Al_2O_3 catalysts and their crystallinity. Temperature programmed reduction (TPR) experiments were performed to determine the reducibility of the surface oxides. Prior to the TPR experiments, the samples were pretreated in a He flow up to 400 °C and kept for 2 h to remove the adsorbed water and other contaminants followed by cooling to 50 °C. The reducing gas containing 5%H_2/Ar mixture was passed over the samples at a flow rate of 30 ml/min, with the heating rate of 10 °C/min upto 800 °C and kept at that temperature for 30 min. The effluent gas was passed over a molecular sieve trap to remove the generated water and analyzed by GC (CSi 200 GC, Cambridge Scientific Instruments Ltd.) equipped with a thermal conductivity detector (TCD).

3. Catalytic Activity Tests

Catalytic activity test was performed in a tubular fixed bed reactor (O.D.=12.7 mm) with a catalyst of 1.0 g. Prior to the reaction, the catalyst was reduced at 450 °C for 4 h in a flow of 8% H_2 balanced with nitrogen. After reduction, the synthesis gas (H_2/CO/CO_2/CH_4= 38/5.7/6/150), which was selected as a model composition for the second adiabatic reactor in Topsoe's Recycle Methanation Process (TREMP™), was fed into the reactor. The following reaction conditions were employed during activity test; T=350 °C; P=20 bar; space velocity (ml/g hr; SV)=12,000. The effluent gas from the reactor was analyzed by an online gas chromatograph employing Porapak Q/Molecular sieve (5A) packed column connected with TCD for the analysis of carbon oxides, hydrogen, methane and using Ar as an internal standard. The carbon conversion and the conversion to CH_4 are calculated using the following equations based on mol%:

$$\text{Carbon conversion (mol\%)} = \frac{[\text{inlet moles of } (CO+CO_2) - \text{outlet moles of } (CO+CO_2)]}{\text{inlet moles of } (CO+CO_2)} \times 100 \quad (1)$$

$$\text{Conversion to } CH_4\text{(mol\%)} = \frac{\text{outlet moles of } CO_4}{\text{inlet moles of } (CO+CO_2)} \times 100 \quad (2)$$

RESULTS AND DISCUSSION

1. Textural Properties of Fresh Catalysts

Textural properties, like BET surface area, pore volume and average pore diameter of the Ni_xFe_{1-x}/Al_2O_3 catalysts supported by Al_2O_3 are summarized in Table 1 and their pore size distribution patterns are shown in Fig. 1. As shown in Table 1, the surface area, pore volume and the average pore diameter of the catalysts show increasing values with increasing Fe content. However, the surface area of commercial γ-alumina (230 m^2/g) is substantially lower than that of the catalysts prepared in this study. From Fig. 1 it is clear that the meso-pore diameter (8-10 nm) of the all catalysts is responsible in the textural parameters. From results of the textural properties, catalytic activity is expected to be higher with the increase of Fe content.

Table 1. Physicochemical properties of Ni_xFe_{1-x}/Al_2O_3 catalysts

Catalyst/ support	BET surface area (m^2/g)	Pore volume (cm^3/g)	Average pore diameter (nm)
$Ni_{0.9}Fe_{0.1}/Al_2O_3$	147.0	0.331	8.0
$Ni_{0.7}Fe_{0.3}/Al_2O_3$	148.7	0.344	7.9
$Ni_{0.5}Fe_{0.5}/Al_2O_3$	150.1	0.371	8.5
$Ni_{0.3}Fe_{0.7}/Al_2O_3$	150.5	0.407	9.3
$Ni_{0.1}Fe_{0.9}/Al_2O_3$	154.3	0.434	9.8

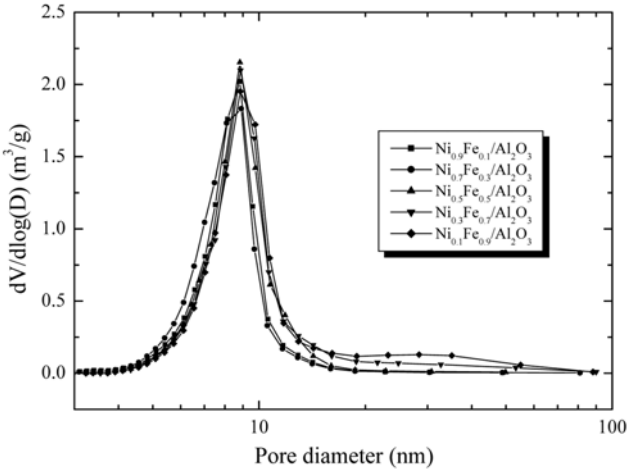

Fig. 1. Pore size distribution of Ni_xFe_{1-x}/Al_2O_3 catalysts.

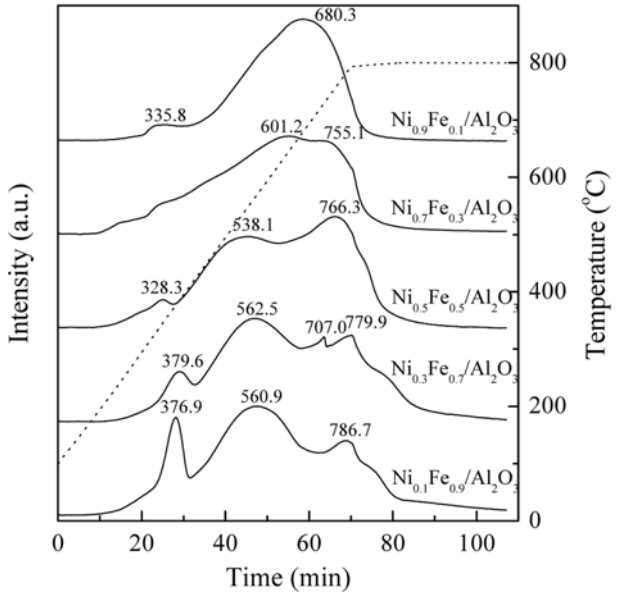

Fig. 2. H_2-TPR profiles of Ni_xFe_{1-x}/Al_2O_3 catalysts.

2. Temperature-programmed Analysis (H_2-TPR)

The reduction of the catalysts was investigated by H_2-TPR. Fig. 2 shows the H_2-TPR profiles of the Ni_xFe_{1-x}/Al_2O_3 catalysts with different Ni (or Fe) contents. The patterns display either two or three important peaks. In the case of $Ni_{0.9}Fe_{0.1}/Al_2O_3$ catalyst with Ni of 90 wt%, the small low temperature peak is overlapped by a large

Table 2. H_2 uptake of Ni_xFe_{1-x}/Al_2O_3 catalysts measured by H_2-TPR

Catalyst	H_2 uptake, mmol H_2/g (degree of reduction, %)		
	Below 450 °C	Above 450 °C	Total
$Ni_{0.9}Fe_{0.1}/Al_2O_3$	0.340 (12.2)	2.442 (87.8)	2.782
$Ni_{0.7}Fe_{0.3}/Al_2O_3$	0.758 (24.2)	2.370 (75.8)	3.128
$Ni_{0.5}Fe_{0.5}/Al_2O_3$	0.801 (22.0)	2.833 (78.0)	3.633
$Ni_{0.3}Fe_{0.7}/Al_2O_3$	0.745 (20.6)	2.872 (79.4)	3.618
$Ni_{0.1}Fe_{0.9}/Al_2O_3$	1.003 (27.3)	2.673 (72.7)	3.676

high temperature peak. In all the patterns the first peak, occurring between 200 to 440 °C, corresponds to the combined reduction of Fe_2O_3 to Fe_3O_4. The second and third peaks, at the high temperature region of 440-800 °C, represent the reduction of Fe_3O_4 to Fe metal and NiO to Ni metal. With increasing Fe content, the high temperature peak is separated into two or three broad peaks, as can be observed from Fig. 2. As shown in Table 2, the reduction degree is 12.2, 24.2, 22.0, 20.6 and 27.3%, for the Fe content of 0.1, 0.3, 0.5, 0.7 and 0.9 respectively. The reduction degree defined as [H_2 consumption below 450 °C/Total H_2 consumption in TPR experiments× 100]. This can be explained as due to the lower reduction temperature of Fe_2O_3 than that of NiO on the Ni_xFe_{1-x}/Al_2O_3 catalysts. But, in the case of Fe_2O_3 catalyst, it is reported that Fe_2O_3 is converted to iron carbide after forming Fe metal [19].

3. The Activity and Selectivity of Ni_xFe_{1-x}/Al_2O_3 Catalysts

The catalytic performance of the Ni_xFe_{1-x}/Al_2O_3 catalysts was measured at 350 °C, 2.0 MPa, 12,000 ml/g_{cat}·h and $H_2/(3CO+4CO_2)$ =1. The activity of catalysts was tested for over 20 h. Fig. 3 shows the variation of conversion with time on stream (TOS) and the relative stability of the catalysts, activity being expressed in terms of percentage conversion of total carbon in CO and CO_2. The carbon conversion was observed to be relatively stable with time on stream for all catalysts. As revealed from the figure, the steady-state activity of the catalysts after a TOS of 20 h varies in the order Fe content=0.1 and 0.3>0.5>0.7>0.9. That is, carbon conversion decreases with increase the Fe content at time on stream of more than 400 min and it correlates with the WGS on iron component. It is well known that Fe-based catalysts show high water gas shift activity (including Fischer-Tropsch synthesis, FTS), and hence iron component is of increasing interest for the FTS than the methanation under the conditions of H_2/CO=2.0, temperature ranges of 250-280 °C, etc. [20]. In the case of Ni-based catalysts, it is well known that they show high methanation activity under the conditions of H_2/CO= 3.0, temperature ranges of 280-600 °C and high WGS activity or deactivation by sintering under the high temperature [21,22]. The Ni metal content also influences the methanation rate of CO or CO_2. Commercially, there are two types of catalysts: the low activity catalyst with Ni composition close to 20 weight percent and a high activity catalyst with Ni composition of 40 weight percent [18,23]. From Fig. 3, it can be observed that the carbon conversion of most catalysts except for Fe content of less than 0.3 was about less than 80%. However, a part of CO converts into CO_2 due to the WGS. Especially, iron-based catalysts under the conditions of H_2/CO=2.0 and

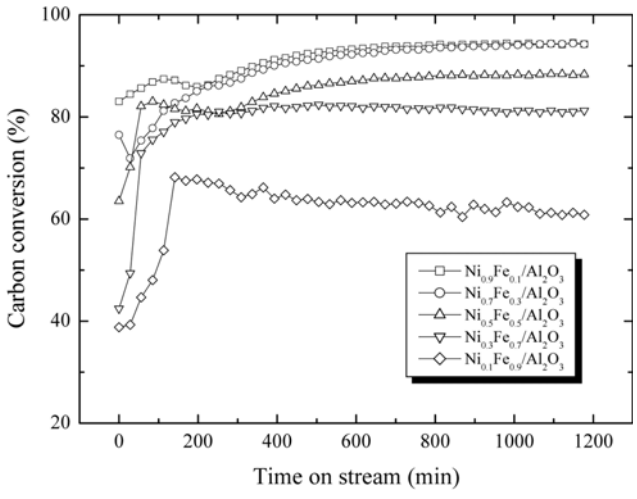

Fig. 3. The CO conversion on Ni_xFe_{1-x}/Al_2O_3 catalysts with time on stream.

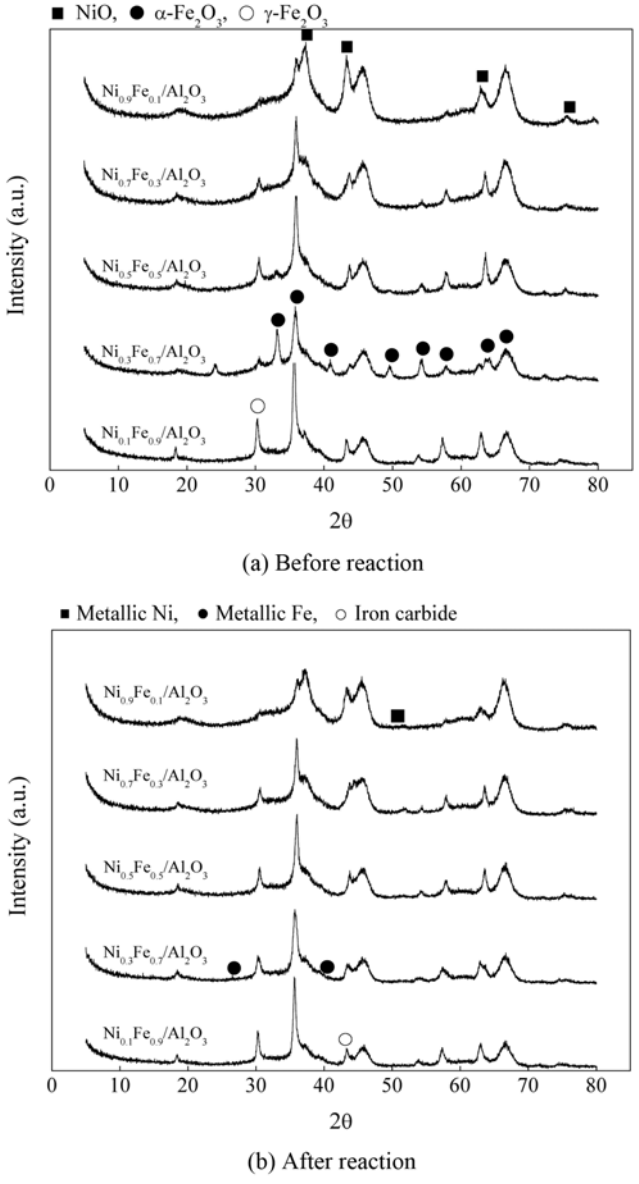

Fig. 4. XRD patterns of Ni_xFe_{1-x}/Al_2O_3 catalysts before and after reaction.

Table 3. The summarized catalytic performance on Ni_xFe_{1-x}/Al_2O_3 catalysts

Catalyst	(CO+CO_2) Conv.	H_2 Conv.	To CH_4 Conv.	Selectivity in products				
				CH_4	H_2	CO	CO_2	By-products[a]
$Ni_{0.9}Fe_{0.1}/Al_2O_3$	94.3	88.5	53.0	56.3	28.5	0	4.4	10.9
$Ni_{0.7}Fe_{0.3}/Al_2O_3$	94.3	88.9	53.5	56.8	27.8	0	4.2	11.2
$Ni_{0.5}Fe_{0.5}/Al_2O_3$	88.4	82.8	41.8	47.3	37.3	0	7.3	8.2
$Ni_{0.3}Fe_{0.7}/Al_2O_3$	81.2	74.1	28.8	35.5	47.3	0	10.0	7.3
$Ni_{0.1}Fe_{0.9}/Al_2O_3$	60.8	53.4	13.0	21.3	61.7	0	14.9	2.0

[a]By-products are the hydrocarbons in the range of C_2-C_5

temperatures of above 300 °C exhibit high CO conversions of the order of 95% with about 33-38% to CO_2 [24].

The activity of Ni_xFe_{1-x}/Al_2O_3 catalysts cannot be explained exactly in terms of ease of reduction, as seen from the data give in Table 2 and by the TPR patterns given in Fig. 2. In co-methanation of CO and CO_2, the methanation of CO_2 is well known to occur more rapidly and selectively than that of CO over Ni-based catalysts [9]. Nevertheless, the adsorption of CO_2 on the clean surface of catalyst is the rate-determining step. Under the existing conditions the rate at high concentrations of CO_2 is controlled probably by the surface reaction or the desorption step [25]. It may be observed from Fig. 3 that the overall carbon conversion decreases with increase in Fe content due to favorable WGS reaction.

To understand further the activity of Ni_xFe_{1-x}/Al_2O_3 catalysts, XRD study was carried out on the catalysts collected before and after reaction. Fig. 4(a) and 4(b) display the XRD patterns of these catalysts. The fresh catalysts prepared by impregnation have shown hematite (α-Fe_2O_3) as the major detectable iron phase with the characteristic peaks appearing at 2θ values of 24.2°, 33.1°, 35.6°, 40.8°, 49.5°, 54.0°, 57.6°, 62.5° and 64.0°, and agreeing with data reported in the JCPDS files [19], as well as the cubic NiO with the characteristic peaks appearing at 2θ values of 37.3°, 43.4° and 62.8°. In Fig. 4(a), the iron peaks show the strong intensity with increasing Fe content. In Fig. 4(b), the catalysts after reaction show peaks of metallic nickel, iron carbide and metallic iron. Particularly, the peak at 44° is a strong indication of the carbide formation [26]. In particular, the peaks around 26° and 52° show faintly the presence of metallic iron and nickel, respectively. However, the oxidation of iron and nickel moieties during the reaction cannot be neglected during the co-methanation of CO and CO_2 from the appearance of the peaks of nickel oxide and iron oxides in Fig. 4(b).

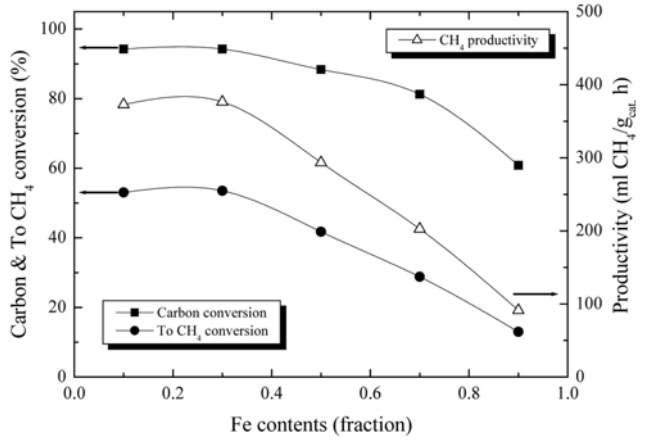

Fig. 5. Carbon conversion and CH_4 productivity on Ni_xFe_{1-x}/Al_2O_3 catalysts according to Fe contents.

The selectivity of the catalysts is presented in Table 3. In addition, carbon conversion and productivity of CH_4 are shown in Fig. 5. The $Ni_{0.7}Fe_{0.3}/Al_2O_3$ catalyst shows the highest selectivity toward CH_4 (56.8%) in the products. On the other hand, the CH_4 selectivity in the $Ni_{0.1}Fe_{0.9}/Al_2O_3$ catalyst (with the highest Fe content) has the lowest value of 21.3%. Also, the increase of Fe contents reduced the carbon conversion as well as the productivity of CH_4, as shown in Fig. 5. This trend relates to the CO_2 formation due to WGS rather than the hydrogenation by iron component of catalyst. The high selectivity towards hydrocarbons (C_2-C_5 by-products) in the case of $Ni_{0.3}Fe_{0.7}/Al_2O_3$ catalyst suggests the predominance of co-methanation over WGS.

CONCLUSION

The Fe content in Ni_xFe_{1-x}/Al_2O_3 catalysts plays a critical role in the activity and CH_4 productivity during the co-methanation of CO and CO_2. The $Ni_{0.7}Fe_{0.3}/Al_2O_3$ catalyst offers higher carbon conversion and CH_4 productivity along with the formation of useful hydrocarbons in the C_2-C_5 range as by-products. High Fe content causes decrease in carbon conversion and CH_4 productivity because of WGS reaction.

ACKNOWLEDGEMENT

This work was supported by Energy Resource R&D program (2009T100100674) under the Ministry of Knowledge Economy, Republic of Korea.

REFERENCES

1. S. A. Bresler and J. D. Ireland, *Chem. Eng.*, **1**, 94 (1972).
2. A. Harms, B. Höhlein, E. Jørn and A. Skov, *Oil Gas J.*, **78**, 120 (1980).
3. J. R. Rostrup-Nielsen, K. Pedersen and J. Sehested, *Appl. Catal. A*, **330**, 134 (2007).
4. S. Takenaka, T. Shimizu and K. Otsuka, *Int. J. Hydrog. Energy*, **29**, 1065 (2004).
5. N. R. Udengaard, A. Olsen and C. Wix-Nielsen, *Pittsburgh Coal Conf.* (2006).
6. A. N. Akin, M. Ataman, A. E. Aksoylu and Z. I. Oensan, *React.*

Kinet. Catal. Lett., **76**, 265 (2002).
7. M. Nawdali and D. Bianchi, *Appl. Catal. A*, **231**, 45 (2002).
8. C. N. Satterfield, *Heterogeneous catalysis in industrial practice*, 2nd Ed., Krieger Publishing, Malabar, FL (1991).
9. S. Fujita, M. Nakamura, T. Doi and N. Takezawa, *Appl. Catal. A*, **104**, 87 (1993).
10. K. B. Kester, E. Zagli and J. L. Falconer, *Appl. Catal.*, **22**, 311 (1986).
11. M. P. Andersson, T. Bligaard, A. L. Kustov, K. E. Larsen, J. Greeley, T. Johannessen, C. H. Christensen and J. K. Nørskov, *J. Catal*., **239**, 501 (2006).
12. J. Sehested, S. Dahl, J. Jacobsen and J. R. Rostrup-Nielsen, *J. Phys. Chem. B*, **109**, 2432 (2005).
13. H. Habazaki, M. Yamasaki, B. P. Zhang, A. Kawashima, S. Kohno, T. Takai and K. Hashimoto, *Appl. Catal. A*, **172**, 131 (1998).
14. T. Ishihara, K. Eguchi and H. Arai, *Appl. Catal*., **30**, 225 (1987).
15. A. L. Kustov, A. M. Frey, K. E. Larsen, T. Johannessen, J. K. Nørskov and C. H. Christensen, *Appl. Catal. A*, **320**, 98 (2007).
16. K. Yaccato, R. Carhart, A. Hagemeyer, A. Lesik, P. Strasser, A. F. Volpe, H. Turner, H. Weinberg, R. K. Grassel and C. Brooks, *Appl. Catal. A*, **296**, 30 (2005).
17. http://www.topsoe.com/research.
18. J. H. Kim, S. H. Kang, J. H. Ryu, S. K. Lee, S. H. Kim, D. Y. Lee, M. H. Kim, Y. D. Yoo, C. D Byun and H. J. Lim, *Korean Chem. Eng. Res*., In press (2011).
19. S. H. Kang, J. W. Bae, P. S. Sai Prasad and K. W. Jun, *Catal. Lett.*, **125**, 264 (2008).
20. R. L. Espinoza, A. P. Steynberg, B. Jager and A. C. Vosloo, *Appl. Catal. A*, **186**, 13 (1999).
21. L. Seglin, *Methanation of synthesis gas*, American Chemical Society (1974).
22. J. R. Rostrup-Nielsen, K. Pedersen and J. Sehested, *Appl. Catal. A*, **330**, 134 (2007).
23. J. Kopyscinski, T. J. Schildhauer and S. M. A. Biollaz, *Fuel*, **89**, 1763 (2010).
24. S. H. Kang, J. W. Bae, J. Y. Cheon, Y. J. Lee, K. S. Ha, K. W. Jun, D. H. Lee and B. W. Kim, *Appl. Catal. B*., **1-2**, 169 (2010).
25. T. Van Herwijnen, H. Vav Doesburg and W. A. De Jong, *J. Catal*., **28**, 391 (1973).
26. W. Ning, N. Koizumi, H. Chang, T. Mochizuki, T. Itoh and M. Yamada, *Appl. Catal. A*, **312**, 35 (2006).